Division of Clinical Pharmaceutics[1]; Department of Pharmacy[2]; Division of Clinical Pharmaceutics and Pharmacy Practice[3]; Division of Gastroenterology[4], Tohoku Medical and Pharmaceutical University; Miyagi, Japan

Fibronectin plays a major role in hypoxia-induced lenvatinib resistance in hepatocellular carcinoma PLC/PRF/5 cells

M. Takahashi[1,2], K. Okada[2,3,*], R. Ouchi[2,3], T. Konno[1,2], K. Usui[2,3], H. Suzuki[1,2], M. Satoh[4], T. Kogure[4], K. Satoh[4], Y. Watanabe[3], H. Nakamura[1], Y. Murai[1]

Received September 1, 2021, accepted October 20, 2021

**Corresponding author: Kouji Okada, Division of Clinical Pharmaceutics and Pharmacy Practice, Tohoku Medical and Pharmaceutical University, 1-12-1 Fukumuro, Miyagino-ku, Sendai, Miyagi, 983-8512, Japan kokada@tohoku-mpu.ac.jp*

Pharmazie 76: 594-601 (2021) *doi: 10.1691/ph.2021.1854*

Resistance to lenvatinib mesylate (LEN), a systemic chemotherapy that can be administered orally, has been a major issue for treatment of hepatocellular carcinoma (HCC). Although HCC is the tumor that most exhibits intratumoral hypoxia, which has been shown to be involved in the development of treatment resistance, there are no reports of LEN resistance in HCC treatment under hypoxia. The purpose of our study was to elucidate the mechanism of treatment resistance to LEN under hypoxia using HCC cell lines. We confirmed LEN resistance under hypoxic conditions in HCC cell lines. There was a significant increase in the IC_{50} value of PLC/PRF/5 cells from 13.0±0.8 μM in normoxia to 21.3±1.1 μM in hypoxia, but in HepG2 cells, the increase was not significant. To elucidate the LEN resistance mechanism of PLC/PRF/5 cells under hypoxia, we performed microarray analysis and extracted genes that are thought to be related to this mechanism. Furthermore, *in-silico* analysis confirmed significant changes in the extracellular matrix, and among them, FN1 encoding fibronectin was determined as the hub of the gene cluster. The expression of fibronectin in PLC/PRF/5 cells examined with immunofluorescence staining was significantly elevated in and outside of cells under hypoxia, and tended to decrease when cells were exposed to LEN under normoxia. Furthermore, the fibronectin concentration in the culture solution of PLC/PRF/5 cells examined by ELISA was 2.3 times higher under hypoxia than under normoxia under LEN(-) conditions, and 1.6 times higher under hypoxia than under normoxia under LEN(+) conditions. It is assumed that in PLC/PRF/5 cells, fibronectin is probably suppressed as an indirect effect of LEN under normoxia, but transcription factors such as HIF-1α are induced under hypoxia, thus enhancing the production of fibronectin and attenuating the effect of LEN, resulting in drug resistance. This behavior of fibronectin with LEN exposure under hypoxia is probably specific to PLC/PRF/5 cells. Further studies should verify the combined effective inhibition of fibronectin and the MAPK pathway as a promising therapeutic strategy to enhance the value of LEN in HCC treatment.

1. Introduction

Liver cancer was the second most common cause of cancer-related deaths in 2020, and hepatocellular carcinoma (HCC) accounts for 75%–85% of liver cancer cases (Sung et al. 2021). The main risk factors for the development of HCC include chronic infection with the hepatitis B virus (HBV) or hepatitis C virus (HCV), ingestion of foods contaminated with aflatoxin, consumption of large amounts of alcohol, obesity, type 2 diabetes, smoking, etc. (Thun et al. 2018). In the past, HBV and HCV were the major causes of HCC, but in recent years, obesity, type 2 diabetes, and non-alcoholic fatty liver disease have been increasing as causes of HCC in many parts of the world (Marengo et al. 2015). The treatment algorithm for HCC is determined according to the disease stage, and the Barcelona Clinic Liver Cancer staging is used as the standard indicator (Waller et al. 2015). Current HCC treatment options include hepatectomy, transarterial chemoembolization, liver ablation, liver transplantation, radiation therapy, and systemic chemotherapy (Waller et al. 2015; Bruix and Llovet 2015; El-Serag et al. 2008). For early stage cancers, hepatectomy, liver ablation, and liver transplantation are recommended, whereas systemic chemotherapy is indicated for advanced stages (EASL Clinical practice Guidelines 2018). Even in patients with early stages of the disease, it is common to eventually shift the treatment to systemic chemotherapy due to the mounting load on the liver from accumulation of treatments and disease progression. The National Comprehensive Cancer Network (NCCN) Guidelines recommend sorafenib tosylate (SFB), lenvatinib mesylate (LEN), and a combination of atezolizumab and bevacizumab as first-line systemic chemotherapy options (NCCN Guideline 2021). In recent years, there has been an increase in the number of drugs available for systemic chemotherapy in patients with HCC, but the treatment options remain limited.

LEN, which is a systemic chemotherapy option for HCC, has demonstrated non-inferiority to SFB, the standard treatment before emergence of LEN, in terms of overall survival in a comparative study (Kudo et al. 2018). In addition, secondary endpoints, i.e., progression-free survival and time to progression, were evaluated based on the Response Evaluation Criteria in Solid Tumor (RECIST) 1.1, which is a criterion that shows the efficacy of an anticancer agent for solid tumors, as well as the modified RECIST (mRECIST), which is a similar standard specific for HCC that adds blood flow assessment to RECIST. According to the evaluation of response rates based on blinded, independent image reviews, LEN was superior to SFB in terms of these secondary endpoints (Kudo et al. 2018). LEN is a multi-target tyrosine kinase inhibitor (TKI) for vascular endothelial growth factor receptor (VEGFR)1-3, fibroblast growth factor (FGFR)1-4, platelet-derived growth factor receptor (PDGFR), rearranged during transfection (RET) fusions, and tyrosine-protein kinase (KIT), and can be administered orally. Targeting angiogenic signals such as VEGFR and FGFR is a rational treatment for HCC because HCC is highly vascularized (Zhu et al. 2008). It has been

shown that LEN inhibits the growth of HCC cells *in vitro* by inactivating the fibroblast growth factor (FGF) signaling pathway and also suppressing the FGF signaling pathway in preclinical human HCC xenograft tumors (Matsuki et al. 2018). Previous studies also demonstrated increased expression of FGF19 and FGFR4 in HCC (Desnoyers et al. 2008); the expression of FGF19 is involved in the progression of HCC (Miura et al. 2012) and the overexpression of FGF19 may induce the onset of HCC (Nicholes et al. 2002). As a result, LEN, which targets the FGFR receptor and suppresses the FGF signaling pathway, is considered to be more clinically useful than SFB. However, resistance development to LEN has been a major issue for HCC, which is already limited in treatment options.

The microenvironment is involved in the development of treatment resistance in solid tumors. Tumor vasculature involved in the supply of nutrients to tumor cells, intratumoral hypoxia involved in the survival mechanism, tumor acidity due to the involvement of the glycolytic system, induction of autophagy due to hypoxia and acidity, drug distribution in the tumor, and tumor regrowth during treatment have been mentioned as factors associated with treatment resistance (Tan et al. 2015). Among these factors, intratumoral hypoxia is known to make it impossible to administer drugs at toxic concentrations, eliminate apoptosis from the loss of the tumor suppressor protein p53, increase angiogenesis and invasiveness, and increase the expression of genes involved in drug resistance, such as the MDR gene that codes for the P-glycoprotein and is involved in the previously mentioned glycolytic system and tumor autophagy (Tan et al. 2015). Advanced HCCs often appear in the form of multiple nodules (Schlageter et al. 2014), and because both normal liver and hepatocytes have high vascular density, tumor cell growth within the nodules consumes large amounts of oxygen and often creates a hypoxic microenvironment (Chen and Lou 2017). HCC is a tumor that most exhibits intratumoral hypoxia, and the median oxygen concentration in tumors is reportedly 0.8% (McKeown 2014). Resistance to SFB treatments for HCC mediated by hypoxia is reported to involve autophagy (Wu et al. 2020) and an increased expression of programmed death receptor-1 (PD-1), which is an immune checkpoint inhibitor target (Chen et al. 2015). It has also been reported that hypoxia inducible factor-1α (HIF-1α) (Semenza 2003), which is widely known as an important transcription factor for the adjustment of proteins connected to cell proliferation, survival, and adhesion; angiogenesis; apoptosis; and sugar metabolism in hypoxia. It is further involved in the increased expression of glucose transporter 1 (GLUT1) and VEGF etc. (Xu et al. 2014; Liang et al. 2013). In addition, studies of human HCC clinical specimens have reported significantly elevated levels of HIF-1α protein in tumors (Dai et al. 2009), with an increased expression associated with a worse prognosis (Yang et al 2014). Elucidation of drug resistance in hypoxia is very important to the successful treatment of patients with HCC. With regards to the treatment resistance of LEN, it has been reported that the hepatocyte growth factor (HGF) attenuates the effect of LEN by reducing its antiproliferative effect, pro-apoptosis, and anti-infiltration effect in cells in which c-MET is highly expressed (Rongdang et al. 2020). Other reports indicate that ETS-1 is involved in LEN resistance mediated by VEGFR (Zhao et al. 2021). However, there are no reports of LEN resistance in HCC treatment under hypoxia. The purpose of our study was to elucidate the mechanism of treatment resistance to LEN under hypoxia using HCC cell lines.

2. Investigations and results

2.1. Lenvatinib dose-response chemosensitivity in PLC/PRF/5 and HepG2 cells

Cell viability was evaluated by the MTS assay for dose response to LEN in normoxia and hypoxia in PLC/PRF/5 and HepG2 cells. LEN inhibited cell proliferation in a dose-dependent manner, but in PLC/PRF/5 cells, we observed resistance to the cell proliferation inhibitory effect of LEN under hypoxia (Fig. 1A). At LEN concentration of 12.5 μM, there was a 47.2% increase in cell viability in PLC/PRF/5 cells under hypoxia relative to the cells under normoxia, whereas in HepG2 cells, there was an increase of 13.2% in cell viability under hypoxia

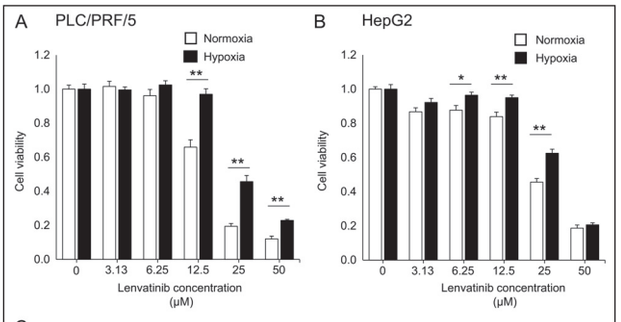

C

LEN IC_{50} (μM)	Normoxia	Hypoxia	*p*	Increase rate of IC_{50} (Hypoxia - Normoxia) / Hypoxia
PLC/PRF/5	13.0± 0.8	21.3± 1.1	< 0.01	**63.8± 3.3 %**
HepG2	23.0± 0.8	26.3± 1.1	N.S.	14.3± 0.9 %

Fig. 1: Hypoxia causes resistance to lenvatinib-induced cytotoxicity, while lenvatinib dose-response effects differ among hepatocellular carcinoma (HCC) cell lines (A) PLC/PRF/5 cells and (B) HepG2 cells seeded on 96-well plates at a density of 1×10^4 cells/well. These cells were incubated with increasing concentrations of lenvatinib for 72h under normoxia (95% air and 5% CO_2) or hypoxia (94 %N_2, 1% O_2 and 5% CO_2) conditions and evaluated for cell viability using the MTS assay. Data are mean±SEM of assays done in triplicate. *p<0.05, **p<0.01 for normoxia *vs* hypoxia conducted by student's t-test. (C) IC_{50} values for lenvatinib in different HCC cell lines were calculated using the JMP 14.2 software.

compared to normoxia (Fig. 1A and 1 B). There was a significant increase in the IC_{50} value of PLC/PRF/5 cells from 13.0±0.8 μM under normoxia to 21.3±1.1 μM under hypoxia. In HepG2 cells, the increase was from 23.0±0.8 μM under normoxia to 26.3±1.1 μM under hypoxia, which was, however, not significant. The rate of increase in IC_{50} under hypoxia relative to normoxia was 63.8±3.3% in PLC/PRF/5 cells and 14.3±0.9% in HepG2 cells, indicating that the increase was more remarkable in PLC/PRF/5 cells (Fig. 1C).

2.2. Comprehensive gene expression analysis of resistance to LEN under hypoxia in PLC/PRF/5 cells

Comprehensive gene analysis was conducted using the total RNA extracted from PLC/PRF/5 cells. Under normoxia, there were 921 downregulated genes with lenvatinib compared to without lenvatinib. Table 1 shows a list of the top 50 most downregulated genes. There were 409

Table 1: List of top 50 the most down-regulated genes with lenvatinib compared to without lenvatinib under normoxia.

RefSeq_id	symbol	description	ratio
XR_942480.1	PGM3	phosphoglucomutase 3	0.16
NM_006931.2	SLC2A3	solute carrier family 2 member 3	0.20
NM_001134.2	AFP	alpha fetoprotein	0.21
NR_046371.1	CP	ceruloplasmin (ferroxidase)	0.21
XM_011522450.1	RAB26	RAB26, member RAS oncogene family	0.23
NM_015303.3	VPS8	VPS8, CORVET complex subunit	0.23
XM_011535916.1	AHI1	Abelson helper integration site 1	0.24
XR_931950.1	PIGB	phosphatidylinositol glycan anchor biosynthesis class B	0.26
XM_011519179.1	WDR34	WD repeat domain 34	0.26
NR_036462.1	APITD1	apoptosis-inducing, TAF9-like domain 1	0.27
NM_000935.2	PLOD2	procollagen-lysine, 2-oxoglutarate 5-dioxygenase 2	0.27
NM_212474.2	FN1	fibronectin 1	0.30
NM_031935.2	HMCN1	hemicentin 1	0.32
XM_011516792.1	NDRG1	N-myc downstream regulated 1	0.33
NM_001402.5	EEF1A1	eukaryotic translation elongation factor 1 alpha 1	0.33
NM_021979.3	HSPA2	heat shock protein family A (Hsp70) member 2	0.33
NM_003670.2	BHLHE40	basic helix-loop-helix family member e40	0.35
NM_016378.3	VCX2	variable charge, X-linked 2	0.36
NM_001127400.1	YPEL5	yippee like 5	0.37

NM_001282663.1	MICAL2	microtubule associated monooxygenase, calponin and LIM domain containing 2	0.38
NM_001317120.1	ZNF331	zinc finger protein 331	0.38
NM_153365.2	TAPT1	transmembrane anterior posterior transformation 1	0.38
NR_002780.1	HIGD2B	HIG1 hypoxia inducible domain family member 2B	0.39
NM_032049.3	AGTR1	angiotensin II receptor type 1	0.40
NM_004354.2	CCNG2	cyclin G2	0.40
XM_005254117.2	ADAM10	ADAM metallopeptidase domain 10	0.41
NM_001301837.1	C12orf57	chromosome 12 open reading frame 57	0.41
NM_001013398.1	IGFBP3	insulin like growth factor binding protein 3	0.41
NM_138391.4	TMEM183A	transmembrane protein 183A	0.42
NM_001063.3	TF	transferrin	0.43
NM_001122839.1	SLC50A1	solute carrier family 50 member 1	0.43
NM_001166451.1	KNG1	kininogen 1	0.43
NM_018004.2	TMEM45A	transmembrane protein 45A	0.43
XM_005244940.3	EFNA1	ephrin-A1	0.43
NM_152288.2	ORAI3	ORAI calcium release-activated calcium modulator 3	0.43
NM_017582.6	UBE2Q1	ubiquitin conjugating enzyme E2Q family member 1	0.43
NM_022735.3	ACBD3	acyl-CoA binding domain containing 3	0.43
XM_006711051.1	TMEM59	transmembrane protein 59	0.45
NM_012180.2	FBXO8	F-box protein 8	0.45
NM_000756.3	CRH	corticotropin releasing hormone	0.45
NM_018433.5	KDM3A	lysine demethylase 3A	0.45
XM_006721903.1	NBR1	neighbor of BRCA1 gene 1	0.46
XM_011517299.1	DERL1	derlin 1	0.46
NM_183065.2	TMEM107	transmembrane protein 107	0.46
NM_001253384.1	RPL15	ribosomal protein L15	0.46
NM_080605.3	B3GALT6	Beta-1,3-galactosyltransferase 6	0.47
NM_001823.4	CKB	creatine kinase, brain	0.47
NM_013332.3	HILPDA	hypoxia inducible lipid droplet associated	0.47
XR_926244.1	TDP2	tyrosyl-DNA phosphodiesterase 2	0.47
NM_001243280.1	ALCAM	activated leukocyte cell adhesion molecule	0.48

genes that were upregulated with lenvatinib under hypoxia compared to with lenvatinib under normoxia. Table 2 shows a list of the top 50 most upregulated genes. Moreover, 200 different genes related to LEN resistance under hypoxia were identified according to the procedures described in the Experimental section. Table 3 shows a list of the top 50 genes that were common to the two experimental conditions and had the highest rate of change. The identified mRNAs belonged mainly to components related to cell composition, such as extracellular exosomes, cell membranes, and membrane-bound vesicles. Gene Ontology (GO) analysis (cell component) using the DAVID bioinformatics tool to determine the functional role of mRNA revealed GO terms primarily associated with the extracellular matrix (ECM) (Fig. 2A). In addition, to interpret the results, the functional interaction network of the identified genes was analyzed using the STRING software, and the FN1 gene encoding the ECM component fibronectin was identified as the hub (Fig. 2B).

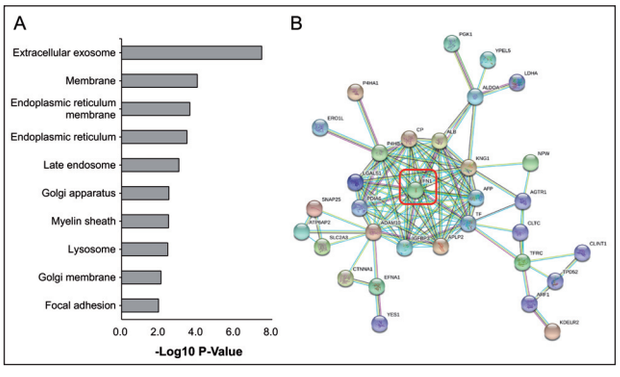

Fig. 2: Global gene expression profiling shows the involvement of the extracellular matrix component, fibronectin, for the resistance of lenvatinib under hypoxia in PLC/PRF/5 cells. (A) Gene Ontology (GO) analysis using DAVID. The representative cell component terms with top ten enrichment scores are presented. The horizontal axis represents the significance (p value) for each term, while the vertical axis represents the GO terms for cell components. (B) Protein-protein interaction network analysis using STRING. FN1 is surrounded by a red frame.

Table 2: List of top 50 the most up-regulated genes with lenvatinib under hypoxia compared to with lenvatinib under normoxia.

RefSeq_id	symbol	description	ratio
XM_011516792.1	NDRG1	N-myc downstream regulated 1	24.37
NM_006931.2	SLC2A3	solute carrier family 2 member 3	15.47
NM_013332.3	HILPDA	hypoxia inducible lipid droplet associated	9.55
NM_001823.4	CKB	creatine kinase, brain	7.03
NM_000935.2	PLOD2	procollagen-lysine, 2-oxoglutarate 5-dioxygenase 2	5.64
XR_942480.1	PGM3	phosphoglucomutase 3	4.72
XM_005244940.3	EFNA1	ephrin-A1	4.62
NM_018004.2	TMEM45A	transmembrane protein 45A	4.52
NM_015303.3	VPS8	VPS8, CORVET complex subunit	4.24
NM_001142595.1	P4HA1	prolyl 4-hydroxylase subunit alpha 1	3.99
XM_011536684.1	ERO1A	endoplasmic reticulum oxidoreductase alpha	3.97
XM_011522450.1	RAB26	RAB26, member RAS oncogene family	3.92
NR_033361.1	TMCC1	transmembrane and coiled-coil domain family 1	3.81
NR_046371.1	CP	ceruloplasmin (ferroxidase)	3.76
NM_003670.2	BHLHE40	basic helix-loop-helix family member e40	3.74
NM_001013398.1	IGFBP3	insulin like growth factor binding protein 3	3.67
XM_011519179.1	WDR34	WD repeat domain 34	3.59
NM_001289910.1	IDH2	isocitrate dehydrogenase 2 (NADP+), mitochondrial	3.58
NM_001292030.1	TTC39C	tetratricopeptide repeat domain 39C	3.47
NM_001001701.3	C4orf3	chromosome 4 open reading frame 3	3.45
NM_001300965.1	CSRP2	cysteine and glycine rich protein 2	3.41
XR_926244.1	TDP2	tyrosyl-DNA phosphodiesterase 2	3.39
XM_011536684.1	ERO1A	endoplasmic reticulum oxidoreductase alpha	3.38
NM_001291737.1	CD24	CD24 molecule	3.34
NM_000756.3	CRH	corticotropin releasing hormone	3.28
NM_001284213.2	CAST	calpastatin	3.14
NR_036462.1	APITD1	apoptosis-inducing, TAF9-like domain 1	3.13
NM_001063.3	TF	transferrin	3.11
NM_001317120.1	ZNF331	zinc finger protein 331	3.06
NM_001122839.1	SLC50A1	solute carrier family 50 member 1	3.06
XM_011540001.1	ALDH18A1	aldehyde dehydrogenase 18 family member A1	3.01
NM_001127400.1	YPEL5	yippee like 5	2.89
NM_001134.2	AFP	alpha fetoprotein	2.83
NM_001005353.2	AK4	adenylate kinase 4	2.81
XM_006718315.1	C11orf49	chromosome 11 open reading frame 49	2.76
NM_004354.2	CCNG2	cyclin G2	2.74
XM_011519493.1	PFKFB3	6-phosphofructo-2-kinase/fructose-2,6-biphosphatase 3	2.73
NM_002305.3	LGALS1	lectin, galactoside-binding, soluble, 1	2.73
NM_000158.3	GBE1	glucan (1,4-alpha-), branching enzyme 1	2.71
NM_000291.3	PGK1	phosphoglycerate kinase 1	2.71
NM_152288.2	ORAI3	ORAI calcium release-activated calcium modulator 3	2.68
XM_011524267.1	LRRC37B	leucine rich repeat containing 37B	2.67
NM_001160094.1	ACOT13	acyl-CoA thioesterase 13	2.62
XM_011509387.1	TMEM9	transmembrane protein 9	2.61
NM_018433.5	KDM3A	lysine demethylase 3A	2.58
NM_001301837.1	C12orf57	chromosome 12 open reading frame 57	2.57
NM_001102426.1	TBC1D8	TBC1 domain family member 8	2.57
NM_212474.2	FN1	fibronectin 1	2.53
NR_033421.1	SLC11A2	solute carrier family 11 member 2	2.49
XR_931950.1	PIGB	phosphatidylinositol glycan anchor biosynthesis class B	2.44

Table 3: List of the top 50 genes that were common to two comparisons and had the highest rate of change. ("Ratio of global normalization value with lenvatinib under hypoxia compared with lenvatinib under normoxia" versus "ratio of global normalization value with lenvatinib as compared to without lenvatinib under normoxia")

RefSeq_id	symbol	description	rate of change
NM_006931.2	SLC2A3	solute carrier family 2 member 3	76.40
XM_011516792.1	NDRG1	N-myc downstream regulated 1	73.82
XR_942480.1	PGM3	phosphoglucomutase 3	30.05
NM_000935.2	PLOD2	procollagen-lysine, 2-oxoglutarate 5-dioxygenase 2	20.56
NM_013332.3	HILPDA	hypoxia inducible lipid droplet associated	20.28
NM_015303.3	VPS8	VPS8, CORVET complex subunit	18.31
NR_046371.1	CP	ceruloplasmin (ferroxidase)	17.55

XM_011522450.1	RAB26	RAB26, member RAS oncogene family	17.13
NM_001823.4	CKB	creatine kinase, brain	14.99
XM_011519179.1	WDR34	WD repeat domain 34	13.89
NM_001134.2	AFP	alpha fetoprotein	13.52
NR_036462.1	APITD1	apoptosis-inducing, TAF9-like domain 1	11.56
XM_005244940.3	EFNA1	ephrin-A1	10.75
NM_003670.2	BHLHE40	basic helix-loop-helix family member e40	10.67
NM_018004.2	TMEM45A	transmembrane protein 45A	10.56
XM_011535916.1	AHI1	Abelson helper integration site 1	9.84
XR_931950.1	PIGB	phosphatidylinositol glycan anchor biosynthesis class B	9.56
NM_001013398.1	IGFBP3	insulin like growth factor binding protein 3	8.90
NM_212474.2	FN1	fibronectin 1	8.51
NM_001317120.1	ZNF331	zinc finger protein 331	8.05
NM_001127400.1	YPEL5	yippee like 5	7.84
NR_033361.1	TMCC1	transmembrane and coiled-coil domain family 1	7.63
XM_011536684.1	ERO1A	endoplasmic reticulum oxidoreductase alpha	7.45
NM_031935.2	HMCN1	hemicentin 1	7.34
NM_001063.3	TF	transferrin	7.31
NM_000756.3	CRH	corticotropin releasing hormone	7.31
NM_001122839.1	SLC50A1	solute carrier family 50 member 1	7.19
NM_001001701.3	C4orf3	chromosome 4 open reading frame 3	7.17
XR_926244.1	TDP2	tyrosyl-DNA phosphodiesterase 2	7.15
NM_004354.2	CCNG2	cyclin G2	6.85
NM_001142595.1	P4HA1	prolyl 4-hydroxylase subunit alpha 1	6.78
NM_001301837.1	C12orf57	chromosome 12 open reading frame 57	6.24
NM_152288.2	ORAI3	ORAI calcium release-activated calcium modulator 3	6.23
XM_011536684.1	ERO1A	endoplasmic reticulum oxidoreductase alpha	5.96
NM_001292030.1	TTC39C	tetratricopeptide repeat domain 39C	5.89
NR_002780.1	HIGD2B	HIG1 hypoxia inducible domain family member 2B	5.79
NM_018433.5	KDM3A	lysine demethylase 3A	5.70
NM_001291737.1	CD24	CD24 molecule	5.65
NM_001289910.1	IDH2	isocitrate dehydrogenase 2 (NADP+), mitochondrial	5.53
NM_021979.3	HSPA2	heat shock protein family A (Hsp70) member 2	5.36
XM_011524267.1	LRRC37B	leucine rich repeat containing 37B	5.35
NM_138391.4	TMEM183A	transmembrane protein 183A	5.33
NM_001300965.1	CSRP2	cysteine and glycine rich protein 2	5.09
XM_011509387.1	TMEM9	transmembrane protein 9	5.07
NM_032049.3	AGTR1	angiotensin II receptor type 1	5.04
NM_001402.5	EEF1A1	eukaryotic translation elongation factor 1 alpha 1	5.02
XR_946695.1	ECHDC2	enoyl-CoA hydratase domain containing 2	4.96
NM_001282663.1	MICAL2	microtubule associated monooxygenase, calponin and LIM domain containing 2	4.95
XM_011519493.1	PFKFB3	6-phosphofructo-2-kinase/fructose-2,6-biphosphatase 3	4.93
NM_002305.3	LGALS1	lectin, galactoside-binding, soluble, 1	4.91

2.3. Expression levels of the HIF1A and FN1 genes in PLC/PRF/5 cells under hypoxic culture conditions

To examine the impact of hypoxia on PLC/PRF/5 cells, we analyzed the level of mRNA expression of the HIF1A gene that encodes for HIF-1α under normoxia and hypoxia. There was a significant increase in HIF1A expression under hypoxia relative to normoxia at 0 h, i.e. after 12-h pre-culture (Fig. 3A). When a similar analysis was conducted on the mRNA expression level of FN1, there was a significant increase in FN1 expression under hypoxia relative to normoxia at each point in time, and the difference was particularly large at 48 h (Fig. 3B).

2.4. Fibronectin fluorescence immunostaining of HCC cell lines and fibronectin quantification in culture solution

Protein expression analysis at 48 h of culture was conducted for fibronectin levels in PLC/PRF/5 cells and HepG2 cells under normoxia and hypoxia. Fluorescence immunostaining analysis showed an increase in the expression of fibronectin in and outside PLC/PRF/5 cells under hypoxia. Furthermore, with LEN exposure, fibronectin expression tended to decrease under both normoxic and hypoxic conditions. In HepG2 cells, however, no significant changes in fibronectin expression levels were observed under either condition

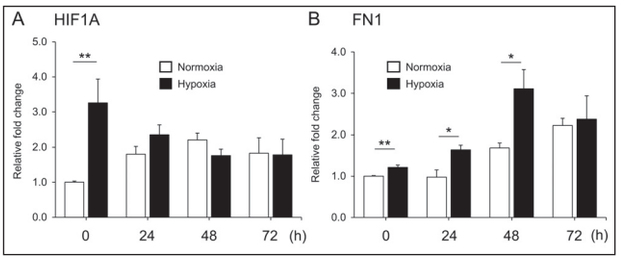

Fig. 3: mRNA expression levels of (A) HIF1A (0 h under normoxia HIF1A/ACTB = 1) and (B) FN1 (0 h under normoxia FN1/ACTB = 1). 0 h refers to the time after 12-h pre-culture. Data are mean ± SEM of duplicate assays. *p<0.05, **p<0.01 for normoxia *vs* hypoxia based on student's t-test.

(Fig. 4A). ELISA-based measurements of fibronectin concentration in the culture solution showed 24.0±1.5 ng/mL and 54.8±7.1 ng/mL under normoxia LEN(-) and hypoxia LEN(-), respectively, in PLC/PRF/5 cells, which meant that the fibronectin concentration increased significantly under hypoxia. Furthermore, the fibronectin concentration was 23.5±8.8 ng/mL and 38.6±7.3 ng/mL under normoxia LEN(+) and hypoxia LEN(+), respectively, indicating that fibronectin expression tended to increase under hypoxia, even in the presence of LEN (Fig. 4B). In HepG2 cells, there was no increase in the fibronectin concentration in the culture solution under hypoxia, and the expression level of fibronectin tended to be lower in general compared to that in PLC/PRF/5 cells (Fig. 4C).

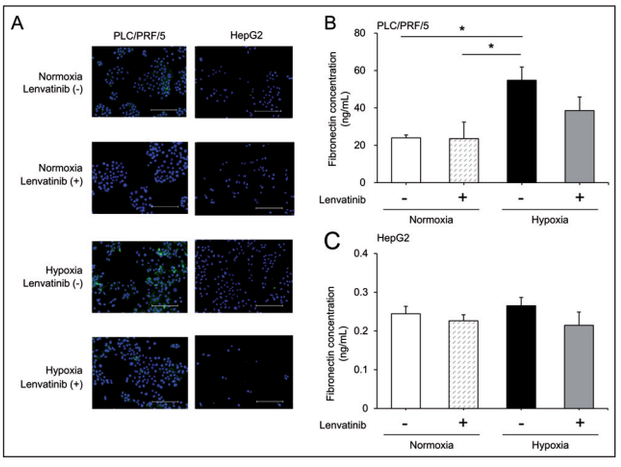

Fig. 4: Fibronectin around PLC/PRF/5 cells and in culture medium is upregulated under hypoxia. (A) The fibronectin localization was analyzed by immunofluorescence staining in PLC/PRF/5 and HepG2 cells. The green color indicates the localization of fibronectin. Nuclei were visualized with DAPI staining in blue. The scale bar represents 200 μm. Fibronectin concentration, using ELISA, in culture medium of (B) PLC/PRF/5 cells and (C) HepG2 cells. Data are mean ± SEM of duplicate measurements. *p<0.05, based on ANOVA followed by Tukey's post-hoc test.

2.5. Effect of LEN on PLC/PRF/5 cells under hypoxia with FN1 knockdown

We examined the effect of LEN on PLC/PRF/5 cells under hypoxia following FN1 knockdown. After transfecting PLC/PRF/5 cells with fibronectin-specific siRNA for 36 h, we observed a significant reduction in the expression levels of the FN1 gene (Fig. 5A). Next, the cells were cultured for 48 h under normoxic and hypoxic conditions with LEN exposure. Compared to normoxic culture, there was a significant improvement in the cell proliferation inhibitory effect of LEN on PLC/PRF/5 cells under hypoxia (Fig. 5B).

2.6. Protein expression analysis of ERK1/2 in PLC/PRF/5 and HepG2 cells

To examine the mechanism of LEN resistance under hypoxia, we used western blotting to analyze the expression of cell survival signal

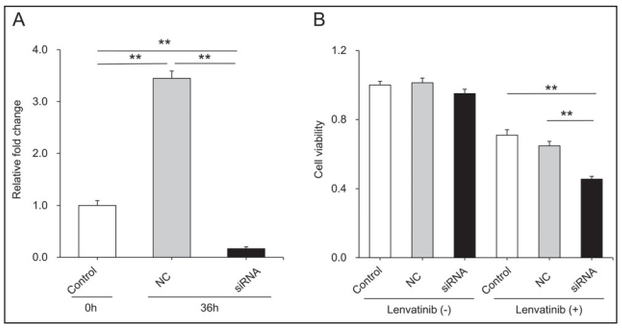

Fig. 5: Knockdown resistance of FN1 to lenvatinib in PLC/PRF/5 cells under hypoxia. (A) FN1 mRNA expression levels 36 h after siRNA knockdown of FN1 in PLC/PRF/5 cells cultured under normoxia compared with negative control siRNA. It is shown by the fold change with the expression levels at 0 h at one. (B) To study the effect of lenvatinib on FN1 knockdown under hypoxia, cell viabilities were examined at 48 h using the MTS assay for PLC/PRF/5 cells cultured under hypoxia with FN1 siRNA or a negative control siRNA. Data are mean ± SEM of duplicate measurements. **p<0.01, based on ANOVA followed by Tukey's post-hoc test. Control:, without transfection reagent; NC, negative control: siRNA; siRNA: FN1 siRNA

protein extracellular signal-regulated kinase 1/2 (ERK1/2) in its whole protein (w-ERK) form and phosphorylated ERK1/2 (p-ERK1/2), its activated protein form. In PLC/PRF/5 cells, p-ERK expression under hypoxia increased at 24 h of culture, and there was an increase in p-ERK1/2 expression with LEN(+) under both normoxia and hypoxia at 48 h of culture (Fig. 6A). When the experiment was conducted using HepG2 cells in the same manner, there was a decrease in p-ERK expression under normoxia LEN(+) and hypoxia LEN(-) compared to normoxia LEN(-) at 24 h of culture, while there was an increase in the expression of p-ERK in both LEN(+) and LEN(-) hypoxia relative to normoxia LEN(-) at 48 h (Fig. 6B).

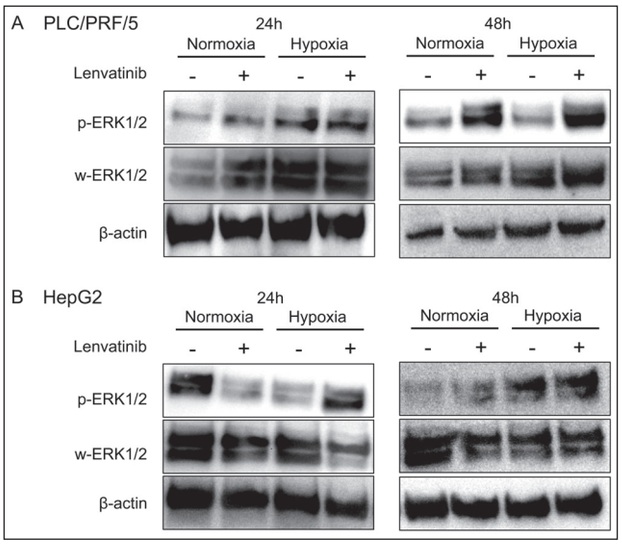

Fig. 6: ERK1/2 is activated under hypoxia in PLC/PRF/5 cells (A) PLC/PRF/5 cells and (B) HepG2 cells for ERK1/2 expression levels using western blot analysis. β-actin was used as a loading control. p-ERK1/2, phospho-ERK1/2; w-ERK, whole ERK1/2

3. Discussion

We confirmed LEN resistance under hypoxic conditions in HCC cell lines. By analyzing the PLC/PRF/5 cell line, which had a large rate of increase in IC_{50} under hypoxia, we showed that ECM such as fibronectin is involved in LEN resistance under hypoxia, and that there is a significant increase in fibronectin expression under hypoxia. Our study is the first to report LEN resistance in HCC cells under hypoxia.

There have already been studies on SFB resistance in PLC/PRF/5cells and HepG2 cells under hypoxia (Xu et al. 2014; Liang et al. 2013). In our study of the effect of LEN under hypoxia, similar trends to the outcome using SFB were observed in PLC/PRF/5 cells, but in HepG2 cells, the rate of increase in IC_{50} of LEN was smaller compared to previous studies on SFB under hypoxia in these cells. It has been reported that PLC/PRF/5 cells exhibit low sensitivity to both SFB and LEN (Matsuki et al. 2018), and the impact of hypoxia may further reduce sensitivity. On the other hand, reports suggest that HepG2 cells are more sensitive to SFB than LEN (Rodríguez-Hernández et al. 2020), which supports our results, where these cells showed low sensitivity to LEN, even under normoxia.

We performed bioinformatics analysis to analyze the mechanism of attenuation of the LEN effect under hypoxia and found that the involvement of fibronectin is important. It has been reported that fibronectin is involved in tumor cell metastasis, radiation resistance, and cell proliferation (Jerhammar et al. 2010), in addition to its roles in normal cells, such as cell adhesion, migration, and wound healing (Aota et al. 1994; Aziz-Seible and Casey 2011; Singh and Schwarzbauer 2012; Veevers-Lowe et al. 2011; Brentnall et al. 2014). Reports indicating that fibronectin was overexpressed in surgically-resected HCC compared to normal hepatocytes (Torbenson et al. 2002) also support that it has a major involvement in HCC. Reports on various cancers, such as gastric cancer and breast cancer, have suggested that ECM such as fibronectin is involved in the resistance to anticancer drugs (Uchihara et al. 2020; Saatci et al. 2020; Yousefi et al. 2021), and studies examining chemotherapy resistance using specimens from cancer patients have also suggested the involvement of ECM (Rossow et al. 2018). In addition, some reports suggest that hypoxia is involved in the regulation of ECM expression (Kakkad et al. 2013; Wang et al. 2019). Our experiments using PLC/PRF/5 cells showed that HIF1A expression levels quickly reached their peak after hypoxic culture, while FN1 expression was most upregulated 48 h after the peak of the HIF1A expression level. Our results support those of previous reports that the expression levels of HIF1A in hepatocellular carcinoma are upregulated within 24 h after hypoxic culture, while the expression levels of FN1 under hypoxia, in another cancer type, were upregulated later than those of HIF1α (Li et al. 2014; Kogita et al. 2014). The expression of fibronectin in PLC/PRF/5 cells examined with immunofluorescence staining was significantly elevated in and outside the cells under hypoxia, and tended to decrease when cells were exposed to LEN under normoxia. Furthermore, the fibronectin concentration in the culture solution of PLC/PRF/5 cells examined by ELISA was 2.3 times higher under hypoxia than under normoxia in LEN(-) conditions, and 1.6 times higher under hypoxia than under normoxia in LEN(+) conditions. Based on these results and taking into consideration the fact that FN1 was extracted by comprehensive gene analysis of PLC/PRF/5 cells as a representative of the group of genes downregulated with LEN exposure under normoxia and upregulated under hypoxia, it is speculated that in PLC/PRF/5 cells, fibronectin is probably suppressed as an indirect effect of LEN under normoxia. However, transcription factors such as HIF-1α are induced under hypoxia, thus enhancing the production of fibronectin and attenuating the effect of LEN, resulting in drug resistance. On the other hand, the expression level of fibronectin in HepG2 cells did not change significantly by either immunofluorescence staining or ELISA analysis of the culture solution. According to a report examining epithelial-mesenchymal transition (EMT) markers in HepG2 or PLC/PRF/5 cells, it has been reported that independent of normoxia and hypoxia, the expression level of vimentin, which is an EMT marker similar to fibronectin, differs greatly between the two cells (Murata et al. 2010). It has also been reported that there is a correlation between the expression of vimentin and fibronectin (Javle et al. 2007, Sudo et al. 2013). From these facts, we speculate that there is a difference in the fibronectin expression level between PLC/PRF/5 and HepG2 cells, and that the behavior of fibronectin under hypoxia is a phenomenon specific to PLC/PRF/5 cells. Given that fibronectin is an important factor in the treatment of LEN under hypoxia, with reference to

the report that the resistance to gemcitabine treatment in the presence of fibronectin in pancreatic cancer cells was overcome by the combined use of the fibronectin inhibitor RGDS (Amrutkar et al. 2019), we conducted a combination treatment experiment of LEN and RGDS under hypoxia using PLC/PRF/5 cells. However, we were unable to show any significant relief of LEN resistance (data not shown). On the other hand, since we showed recovery of the LEN effect under hypoxia by FN1 knockdown in PLC/PRF/5 cells, efficiently inhibiting fibronectin in HCC, which has the property of PLC/PRF/5 cells where fibronectin production increases under hypoxia, may be an important treatment strategy for overcoming LEN resistance under hypoxia.

Furthermore, we analyzed the protein expression of ERK1/2, a key signaling molecule of mitogen-activated protein kinase (MAPK), which is known to be an important signaling pathway for cell proliferation. ERK1/2 is known as a downstream protein of FGFR, which is the site of action of LEN. Reports indicate that p-ERK1/2, the activated protein of ERK1/2, was downregulated by the action of LEN in experiments that used HCC cell lines Hep3B2.1-7 and Huh-7 (Hoshi et al. 2019). In PLC/PRF/5 cells, we confirmed the increase in p-ERK1/2 expression under hypoxia after 24 h of culture. Hypoxia activates ERK, which is known to upregulate HIF-1α (Minet et al. 2000). Considering that ERK1/2 is activated by phosphorylation and is involved in cell functions such as cell proliferation, differentiation, survival, and cell death by phosphorylating various substrates, including transcription factors (Cargnello et al. 2015), it is presumed that the activation of ERK1/2 observed under hypoxia in PLC/PRF/5 cells further affects downstream intracellular processes and contributes to the activation of HIF-1α and the upregulation of fibronectin. Meanwhile, an increased expression of p-ERK1/2 in the LEN-exposed group was confirmed under normoxia and hypoxia at 48 h of culture, which was unexpected. When nilotinib, a TKI, was allowed to act on prostate cancer, upregulation of p-ERK1/2 was observed at the same time as cell proliferation suppression (Schneider et al. 2015). In PLC/PRF/5 cells, unlike LEN-sensitive Hep3B 2.1-7 and Huh-7 cells, the main target of action of LEN is not the suppression of the MAPK pathway, but rather bringing about a paradoxical action on this pathway. It is possible that p-ERK1/2 was activated in the presence of LEN to compensate for the suppression of other pathways. The combination of SFB and MAPK inhibitors on HCC cell lines improves the response of SFB-sensitive cells, and p-ERK has been reported to be a biomarker for drug efficacy (Wang et al. 2018). Thus, the combined use of LEN and MAPK inhibitors may be effective for HCC, which tends to activate ERK upon exposure to LEN. The behavior of p-ERK1/2 in HepG2 cells was different from that seen in PLC/PRF/5 cells, and an increased expression was confirmed under hypoxia at 48 h of culture. The expression pattern of p-ERK at 48 h for HepG2 cells was similar to that at 24 h for PLC/PRF/5 cells. Previous studies examining the resistance of HepG2 cells to chemotherapy due to hypoxia have reported that the expression of p-ERK peaks 48 h after the start of hypoxic culture (Zhu et al. 2012). Combined with our results, we infer that the upregulation of p-ERK by hypoxia in HepG2 cells occurs later than that of PLC/PRF/5. The results showed the diversity of responses by cytomas.

In this study, we used HCC cell lines and confirmed resistance to LEN under hypoxia, suggesting that ECM fibronectin plays an important role in the mechanism of LEN resistance induced under hypoxia in PLC/PRF/5 cells. We believe that the effective suppression of fibronectin will make a significant contribution to LEN treatment for HCC, where fibronectin production is increased. At the same time, the combined effective inhibition of the MAPK pathway is anticipated to become a promising therapeutic strategy that enhances the value of LEN in HCC treatment, and this needs to be verified.

4. Experimental

4.1. Cell lines and cell culture

Two HCC cell lines, PLC/PRF/5 and HepG2, were obtained from the Cell Resource Center for Biomedical Research, Tohoku University (Sendai, Japan). The cell lines were cultured in high-glucose DMEM (Gibco, Grand Island, NY, USA) containing 10% fetal bovine serum (FBS, Gibco). The cells were incubated under normoxia (95% atmosphere and 5% CO_2) or hypoxia (94% N_2, 5% CO_2, 1% O_2) at 37 °C.

4.2. Cell proliferation assay

Cells (1×10^4 cells/well) were seeded in 96-well plates and cultured overnight under normoxia or hypoxia. Next, the cells were treated with 1:2 serial dilutions of lenvatinib mesylate (Funakoshi, Tokyo, Japan) or vehicle (DMSO). After further incubation for 72 h under normoxia or hypoxia, CellTiter 96® Aqueous One Solution Cell Proliferation Assay (Promega, WI, USA) was used to measure cell viability; 20 μL of MTS ([3-(4,5-dimethylthiazol-2-yl)-5-(3carboxymethoxyphenyl)-2-(4-sulfophenyl)-2H-tetrazolium, inner salt) reagent was added to each well and the optical density (OD) at a wavelength of 490 nm was measured. Cells cultured in DMSO served as controls. The inhibition rate was calculated according to the following formula: experimental OD value/control OD value × 100%. The data are presented as the mean±standard error of the mean (SEM); three independent experiments were performed.

4.3. Microarray analysis

PLC/PRF/5 cells on a 60 mm dish at a density of 5×10^5 cells were pre-incubated for 12 h under normoxia or hypoxia. After addition of 17.5 μM LEN, the cells were further incubated for 72 h under normoxia or hypoxia conditions. Total RNA was extracted from PLC/PRF/5 cells using TRIzol reagent (Invitrogen, Carlsbad, CA, USA). Global mRNA profiling was performed using Toray's 3D-Gene mRNA oligo chip v.16 (Toray Industries, Tokyo, Japan). After incubation with RNA samples, the chips were stringently washed, and fluorescence signals were scanned with a 3D-Gene Scanner 3000 and analyzed using 3D-Gene Extraction software. The expression levels of each mRNA were normalized using the background-subtracted signal intensity of all mRNAs in each microarray. To investigate the molecular genetic factors that attenuate the effect of LEN under hypoxia, the mRNA list was created using the following procedure. The experiments were performed on genes that show a value that is at least four times the median global normalization of the vehicle control. First, we identified mRNAs whose global normalization values decreased more than 1.5-fold following exposure to LEN under normoxia compared to vehicle controls under normoxia. We then identified mRNAs whose global normalization values were increased more than 1.5-fold after LEN exposure under normoxia compared to LEN exposure under hypoxia. Finally, common mRNAs for each comparison were extracted, which we used for the subsequent analyses.

4.4. Quantitative real-time PCR (q-RT-PCR)

PLC/PRF/5 cells on a 60 mm dish at a density of 5×10^5 cells were pre-incubated for 12 h under normoxia or hypoxia and further incubated for 0-72 h under normoxia or hypoxia. Total RNA was collected as described above, and cDNA was reverse-transcribed using the High-Capacity RNA-to-cDNA™ Kit according to the manufacturer's instructions (Thermo Fisher Scientific, MA, USA). Real-time RT-PCR was performed using PowerUp™ SYBR™ Green Master Mix (Thermo Fisher Scientific, MA, USA). The following primers were used: FN1, forward, 5-AGGACTGGCATTCACTGATGTG-3 and reverse, 5-GTCACCCTGTACCTGGAAACTTG-3; HIF1A, forward, 5-GCAGAATGCTCAGAGAAAGCG-3 and reverse, 5-TAGCTGCATGATCGTCTGGC-3′. ACTB, forward, 5-CGTCTTCCCCTCCATCGTG-3 and reverse, 5-TCGTCGCCCACATAGGAATC-3′.

4.5. Gene ontology functional enrichment analysis and protein-protein interaction analysis

DAVID 6.8 Bioinformatics Resource (https://david.ncifcrf.gov/) (Dennis et al. 2003; Huang et al. 2009) was used for Gene Ontology (GO). In our study, analysis of significantly enriched biological process GO terms of the identified differentially expressed genes was performed. The protein-protein interaction network was established using the STRING (https://string-db.org/) online search tool (Szklarczyk et al. 2019). For the STRING analysis, a medium-confidence protein interaction score of 0.4 was used.

4.6. Immunofluorescence microscopy

To study the expression of fibronectin, fibronectin staining was performed on PLC/PRF/5 and HepG2 cells. Cells were grown on chamber slides at a density of 5×10^5 cells/well under normoxia for 12 h. Thereafter, PLC/PRF/5 cells were treated with 17.5 μM LEN, and HepG2 cells were treated with 25 μM LEN under normoxia or hypoxia for 48 h. Cells were washed with PBS, fixed with 4% paraformaldehyde, permeabilized with 0.5% Triton X-100 in PBS, and pre-treated with blocking solution. After fixation and blocking of non-specific binding, the chamber slide was incubated with rabbit fluorescently labeled anti-fibronectin antibodies (Alexa Fluor® 488 Anti-Fibronectin, Abcam plc.) at room temperature for 1 h, while protected from light. Then, DAPI-containing antifade reagent (Fluoro-KEEPER®, Nacalai Tesque Inc.) was added to the glass slide. The preparations were analyzed using a fluorescence microscope (Keyence, BZ-X700, Osaka, Japan).

4.7. ELISA

PLC/PRF/5 or HepG2 cells on a 100 mm dish at a density of 2×10^6 cells were pre-incubated for 12 h under normoxia, PLC/PRF/5 cells were treated with 17.5 μM LEN, and HepG2 cells were treated with 25 μM LEN under normoxia or hypoxia for 48 h, and then fibronectin expression levels in the cell culture supernatants were evaluated. ELISA was performed according to the procedure described in the Human Fibronectin Kit (R&D, MN, USA). Briefly, 100 μL of standard human fibronectin or cell culture supernatant (after dilution 100× in the kit assay buffer) was added to the ELISA plate, followed by 50 μL of each human fibronectin antibody solution. The plate was then incubated at room temperature for 2 h in a microplate shaker. Next, all the contents were decanted, the plate washed four times with the kit wash buffer, and

200 µL of human fibronectin conjugate was added. The plate was further incubated at room temperature for 2 h in the microplate shaker. After decanting all the contents, the plate was washed four times with the kit wash buffer, and 200 µL of the substrate solution was added. A stop solution of 50 µL 2 N sulfuric acid was added next. The optical density of each well in the plate was determined using a microplate reader set at a wavelength of 450 nm.

4.8. Small interfering RNA transfection

Small interfering RNA (siRNA) duplexes against human fibronectin (sc-29315) and non-targeting siRNA (sc-36869) were obtained from Santa Cruz (TX, USA) siRNA collection. PLC/PRF/5 cells were seeded at a density of 1×10^4 cells/well in 96 well plates and transfected with 1 nM siRNA using INTERFERin transfection reagent (Polyplus, Illkirch, France) according to the manufacturer's protocol. After 36 h, the cells were processed for further experiments.

4.9. Western blotting

PLC/PRF/5 or HepG2 cells at a density of 2×10^6 cells, on a 100-mm dish, were pre-incubated for 12 h under normoxia. Next, PLC/PRF/5 and HepG2 cells were treated with 17.5 µM and 25 µM LEN, respectively, under normoxia or hypoxia for 48 h. Cells were lysed with M-PER™ Mammalian Protein Extraction Reagent (Thermo Fisher Scientific, MA, USA) with proteinase inhibitors (Santa Cruz Biotechnology, TX, USA). Protein concentrations were measured using a BCA protein assay kit (Fuji Film, Tokyo, Japan). Equal amounts of protein (20 µg) were separated by sodium dodecyl sulfate (SDS)– polyacrylamide gel electrophoresis (PAGE) (4 %–12% standard gel) at a constant voltage of 150 V for 50 min. Western blot analysis was performed according to standard protocols. Proteins were blotted onto polyvinylidene difluoride (PVDF) membranes (Bio-Rad, CA, USA) at a constant voltage of 24 V for 30 min. Subsequently, the membrane was blocked with Blocking One-P (Nacalai Tesque, Kyoto, Japan) overnight at 4 °C. The membrane was then washed using tris-buffered saline with 0.1% Tween 20 detergent (TBS-T) and incubated with primary antibodies that were labeled with p44/42 MAPK (ERK1/2) (CST, MA, USA; Cat. #9102), phospho-p44/42 MAPK (p-ERK1/2) (CST, MA, USA; Cat. #9101), and β-actin (CST, MA, USA; Cat. #4967) at room temperature for 1 h while protected from light. Thereafter, the membrane was incubated with a secondary antibody at room temperature for 1 h in the dark. The antibody concentration was 1:1000 (primary antibody) and 1:5000 (secondary antibody) in TBS-T. The blots were detected using ECL prime western blotting detection reagents (Amersham cytiva, Tokyo, Japan). Chemiluminescent bands were visualized using Lumino Graph III (ATTO, Tokyo, Japan) and Image J 1.53 (http://imagej.nih.gov/ij).

4.10. Statistical analysis

JMP 14.2 (SAS Institute, NC, USA) was used for the analysis. Data were analyzed by ANOVA followed by Tukey's post-hoc test or Student's t-test. Statistical significance was set at $p < 0.05$.

Acknowledgements: This study was supported by the JSPS KAKENHI Grant (No. 21K15558) and the: NISHINOMIYA Basic Research Fund (Japan).

Conflicts of interest: The authors declare no conflict of interest.

References

Amrutkar M, Aasrum M, Verbeke CS, Gladhaug IP (2019) Secretion of fibronectin by human pancreatic stellate cells promotes chemoresistance to gemcitabine in pancreatic cancer cells. BMC Cancer 19: 596.

Aota S, Nomizu M, Yamada KM (1994) The short amino acid sequence Pro-His-Ser-Arg-Asn in human fibronectin enhances cell-adhesive function. J Biol Chem 269: 24756–24761.

Aziz-Seible RS, Casey CA (2011) Fibronectin: functional character and role in alcoholic liver disease. World J Gastroenterol 17: 2482–2499.

Benson AB, D'Angelica MI, Abbott DE, Anaya DA, Anders R, Are C, Bachini M, Borad M, Brown D, Burgoyne A, Chahal P, Chang DT, Cloyd J, Covey AM, Glazer ES, Goyal L, Hawkins WG, Iyer R, Jacob R, Kelley RK, Kim R, Levine M, Palta M, Park JO, Raman S, Reddy S, Sahai V, Schefter T, Singh G, Stein S, Vauthey JN, Venook AP, Yopp A, McMillian NR, Hochstetler C, Darlow SD (2021) Hepatobiliary Cancers, Version 2.2021, NCCN Clinical Practice Guidelines in Oncology J Natl Compr Canc Netw 19: 541–565.

Brentnall M, Weir DB, Rongvaux A, Marcus AI, Boise LH (2014) Procaspase-3 regulates fibronectin secretion and influences adhesion, migration and survival independently of catalytic function. J Cell Sci 127: 2217–2226.

Bruix J, Llovet JM (2002) Prognostic prediction and treatment strategy in hepatocellular carcinoma. Hepatology 35: 519–524.

Cargnello M, Roux PP (2011) Activation and function of the MAPKs and their substrates, the MAPK-activated protein kinases. Microbiol Mol Biol Rev 75: 50–83.

Chen C, Lou T (2017) Hypoxia inducible factors in hepatocellular carcinoma. Oncotarget 8: 46691–46703.

Chen Y, Ramjiawan RR, Reiberger T, Ng MR, Hato T, Huang Y, Ochiai H, Kitahara S, Unan EC, Reddy TP, Fan C, Huang P, Bardeesy N, Zhu AX, Jain RK, Duda DG (2015) CXCR4 inhibition in tumor microenvironment facilitates anti-programmed death receptor-1 immunotherapy in sorafenib-treated hepatocellular carcinoma in mice. Hepatology 6: 1591–1602.

Dai CX, Gao Q, Qiu SJ, Ju MJ, Cai MY, Xu YF, Zhou J, Zhang BH, Fan J (2009) Hypoxia-inducible factor-1 alpha, in association with inflammation, angiogenesis and MYC, is a critical prognostic factor in patients with HCC after surgery. BMC Cancer 9: 418.

Dennis G Jr, Sherman BT, Hosack DA, Yang J, Gao W, Lane HC, Lempicki RA (2003) DAVID: Database for Annotation, Visualization, and Integrated Discovery. Genome Biol 4: P3.

Desnoyers LR, Pai R, Ferrando RE, Hötzel K, Le T, Ross J, Carano R, D'Souza A, Qing J, Mohtashemi I, Ashkenazi A, French DM (2008) Targeting FGF19 inhibits tumor growth in colon cancer xenograft and FGF19 transgenic hepatocellular carcinoma models. Oncogene 27: 85–97.

El-Serag HB, Marrero JA, Rudolph L, Reddy KR (2008) Diagnosis and treatment of hepatocellular carcinoma. Gastroenterology 134: 1752–1763.

European Association for the Study of the Liver (2018) EASL Clinical Practice Guidelines: Management of hepatocellular carcinoma. J Hepatol 69: 182-236.

Fu R, Jiang S, Li J, Chen H, Zhang X (2020) Activation of the HGF/c-MET axis promotes lenvatinib resistance in hepatocellular carcinoma cells with high c-MET expression. Med Oncol 37: 24.

Hoshi T, Watanabe Miyano S, Watanabe H, Sonobe RMK, Seki Y, Ohta E, Nomoto K, Matsui J, Funahashi Y (2019) Lenvatinib induces death of human hepatocellular carcinoma cells harboring an activated FGF signaling pathway through inhibition of FGFR-MAPK cascades. Biochem Biophys Res Commun 513: 1–7.

Huang da W, Sherman BT, Lempicki RA (2009) Systematic and integrative analysis of large gene lists using DAVID bioinformatics resources. Nat Protoc 4: 44–57.

Javle MM, Gibbs JF, Iwata KK, Pak Y, Rutledge P, Yu J, Black JD, Tan D, Khoury T (2007) Epithelial-mesenchymal transition (EMT) and activated extracellular signal-regulated kinase (p-Erk) in surgically resected pancreatic cancer. Ann Surg Oncol 14: 3527–3533.

Jerhammar F, Ceder R, Garvin S, Grénman R, Grafström RC, Roberg K (2010) Fibronectin 1 is a potential biomarker for radioresistance in head and neck squamous cell carcinoma. Cancer Biol Ther 10: 1244–1251.

Kakkad SM, Penet MF, Akhbardeh A, Pathak AP, Solaiyappan M, Raman V, Leibfritz D, Glunde K, Bhujwalla ZM (2013) Hypoxic tumor environments exhibit disrupted collagen I fibers and low macromolecular transport. PLoS One 8: e81869.

Kogita A, Togashi Y, Hayashi H, Sogabe S, Terashima M, De Velasco MA, Sakai K, Fujita Y, Tomida S, Takeyama Y, Okuno K, Nakagawa K, Nishio K (2014) Hypoxia induces resistance to ALK inhibitors in the H3122 non-small cell lung cancer cell line with an ALK rearrangement via epithelial-mesenchymal transition. Int J Oncol 45: 1430–1436.

Kudo M, Finn RS, Qin S, Han KH, Ikeda K, Piscaglia F, Baron A, Park JW, Han G, Jassem J, Blanc JF, Vogel A, Komov D, Evans TRJ, Lopez C, Dutcus C, Guo M, Saito K, Kraljevic S, Tamai T, Ren M, Cheng AL (2018) Lenvatinib versus sorafenib in first-line treatment of patients with unresectable hepatocellular carcinoma: a randomised phase 3 non-inferiority trial. Lancet 391: 1163–1173.

Liang Y, Zheng T, Song R, Wang J, Yin D, Wang L, Liu H, Tian L, Fang X, Meng X, Jiang H, Liu J, Liu L (2013) Hypoxia-mediated sorafenib resistance can be overcome by EF24 through Von Hippel-Lindau tumor suppressor-dependent HIF-1α inhibition in hepatocellular carcinoma. Hepatology 57: 1847–1857.

Li F, Yang R, Zhang X, Liu A, Zhao Y, Guo Y (2014) Silencing of hypoxia-inducible adrenomedullin using RNA interference attenuates hepatocellular carcinoma cell growth in vivo. Mol Med Rep 10: 1295–1302.

London WT, Petrick JL, McGlynn KA (2017) Liver cancer. In: Thun M, Linet MS, Cerhan JR, Haiman CA, Schottenfeld D (ed.) Cancer epidemiology and prevention, 4th ed., New York, p. 635-660

Marengo A, Rosso C, Bugianesi E (2016) Liver cancer: connections with obesity, fatty liver, and cirrhosis. Annu Rev Med 67: 103–117.

Matsuki M, Hoshi T, Yamamoto Y, Ikemori-Kawada M, Minoshima Y, Funahashi Y, Matsui J (2018) Lenvatinib inhibits angiogenesis and tumor fibroblast growth factor signaling pathways in human hepatocellular carcinoma models. Cancer Med. 7: 2641–2653.

McKeown SR (2014) Defining normoxia, physoxia and hypoxia in tumours-implications for treatment response. Br J Radiol 87: 20130676.

Minet E, Arnould T, Michel G, Roland I, Mottet D, Raes M, Remacle J, Michiels C (2000) ERK activation upon hypoxia: involvement in HIF-1 activation. FEBS Lett 468: 53–58.

Miura S, Mitsuhashi N, Shimizu H, Kimura F, Yoshidome H, Otsuka M, Kato A, Shida T, Okamura D, Miyazaki M (2012) Fibroblast growth factor 19 expression correlates with tumor progression and poorer prognosis of hepatocellular carcinoma. BMC Cancer 12: 56.

Murata K, Suzuki H, Okano H, Oyamada T, Yasuda Y, Sakamoto A (2010) Hypoxia-induced des-gamma-carboxy prothrombin production in hepatocellular carcinoma. Int J Oncol 36: 161–170.

Nicholes K, Guillet S, Tomlinson E, Hillan K, Wright B, Frantz GD, Pham TA, Dillard-Telm L, Tsai SP, Stephan JP, Stinson J, Stewart T, French DM (2002) A mouse model of hepatocellular carcinoma: ectopic expression of fibroblast growth factor 19 in skeletal muscle of transgenic mice. Am J Pathol 160: 2295–2307.

Rodríguez-Hernández M A, Chapresto-Garzón R, Cadenas M, Navarro-Villarán E, Negrete M, Gómez-Bravo MA, Victor VM, Padillo FJ, Muntané J (2020) Differential effectiveness of tyrosine kinase inhibitors in 2D/3D culture according to cell differentiation, p53 status and mitochondrial respiration in liver cancer cells. Cell Death Dis 11: 339.

Rossow L, Veitl S, Vorlová S, Wax JK, Kuhn AE, Maltzahn V, Upcin B, Karl F, Hoffmann H, Gätzner S, Kallius M, Nandigama R, Scheld D, Irmak S, Herterich S, Zernecke A, Ergün S, Henke E (2018) LOX-catalyzed collagen stabilization is a proximal cause for intrinsic resistance to chemotherapy. Oncogene 37: 4921–4940.

Saatci O, Kaymak A, Raza U, Ersan PG, Akbulut O, Banister CE, Sikirzhytski V, Tokat UM, Aykut G, Ansari SA, Dogan HT, Dogan M, Jandaghi P, Isik A, Gundogdu F, Kosemehmetoglu K, Dizdar O, Aksoy S, Akyol A, Uner A, Buckhaults PJ, Riazalhosseini Y, Sahin O (2020) Targeting lysyl oxidase (LOX) overcomes chemotherapy resistance in triple negative breast cancer. Nat Commun 11: 2416.

Schlageter M, Terracciano LM, D'Angelo S, Sorrentino P (2014) Histopathology of hepatocellular carcinoma. World J Gastroenterol 20: 15955–15964.

Schneider M, Korzeniewski N, Merkle K, Schüler J, Grüllich C, Hadaschik B, Hohenfellner M, Duensing S (2015) The tyrosine kinase inhibitor nilotinib has antineoplastic activity in prostate cancer cells but up-regulates the ERK survival signal-Implications for targeted therapies. Urol Oncol 33:72. e1-7.

Semenza GL (2003) Targeting HIF-1 for cancer therapy. Nat Rev Cancer 3: 721–732.

Singh P, Schwarzbauer JE (2012) Fibronectin and stem cell differentiation – lessons from chondrogenesis. J Cell Sci 125: 3703–3712.

Sudo T, Iwaya T, Nishida N, Sawada G, Takahashi Y, Ishibashi M, Shibata K, Fujita H, Shirouzu K, Mori M, Mimori K (2013) Expression of mesenchymal markers vimentin and fibronectin: the clinical significance in esophageal squamous cell carcinoma. Ann Surg Oncol 3: S324–S335.

Sung H, Ferlay J, Siegel RL, Laversanne M, Soerjomataram I, Jemal A, Bray F (2021) Global cancer statistics 2020: GLOBOCAN estimates of incidence and mortality worldwide for 36 cancers in 185 countries. CA Cancer J Clin 71: 209–249.

Szklarczyk D, Gable AL, Lyon D, Junge A, Wyder S, Huerta-Cepas J, Simonovic M, Doncheva NT, Morris JH, Bork P, Jensen LJ, von Mering C (2019) STRING v11: protein-protein association networks with increased coverage, supporting functional discovery in genome-wide experimental datasets. Nucleic Acids Res 47(D1): D607–D613.

Tan Q, Saggar JK, Yu M, Wang M, Tannock IF (2015) Mechanisms of drug resistance related to the microenvironment of solid tumors and possible strategies to inhibit them. Cancer J 21: 254–262.

Torbenson M, Wang J, Choti M, Ashfaq R, Maitra A, Wilentz RE, Boitnott J (2002) Hepatocellular carcinomas show abnormal expression of fibronectin protein. Mod Pathol 15: 826–830.

Uchihara T, Miyake K, Yonemura A, Komohara Y, Itoyama R, Koiwa M, Yasuda T, Arima K, Harada K, Eto K, Hayashi H, Iwatsuki M, Iwagami S, Baba Y, Yoshida N, Yashiro M, Masuda M, Ajani JA, Tan P, Baba H, Ishimoto T (2020) Extracellular vesicles from cancer-associated fibroblasts containing annexin A6 induces FAK-YAP activation by stabilizing β1 integrin, enhancing drug resistance. Cancer Res 80: 3222–3235.

Veevers-Lowe J, Ball SG, Shuttleworth A, Kielty CM (2011) Mesenchymal stem cell migration is regulated by fibronectin through α5β1-integrin-mediated activation of PDGFR-β and potentiation of growth factor signals. J Cell Sci 124: 1288–1300.

Waller LP, Deshpande V, Pyrsopoulos N (2015) Hepatocellular carcinoma: A comprehensive review. World J Hepatol 7: 2648–2663

Wang C, Jin H, Gao D, Lieftink C, Evers B, Jin G, Xue Z, Wang L, Beijersbergen RL, Qin W, Bernards R (2018) Phospho-ERK is a biomarker of response to a synthetic lethal drug combination of sorafenib and MEK inhibition in liver cancer. J Hepatol 69: 1057–1065.

Wang WY, Twu CW, Liu YC, Lin HH, Chen CJ, Lin JC (2019) Fibronectin promotes nasopharyngeal cancer cell motility and proliferation. Biomed Pharmacother 109: 1772–1784.

Wu H, Wang T, Liu Y, Li X, Xu S, Wu C, Zou H, Cao M, Jin G, Lang J, Wang B, Liu B, Luo X, Xu C (2020) Mitophagy promotes sorafenib resistance through hypoxia-inducible ATAD3A dependent Axis. J Exp Clin Cancer Res 39: 274.

Xu H, Zhao L, Fang Q, Sun J, Zhang S, Zhan C, Liu S, Zhang Y (2014) MiR-338-3p inhibits hepatocarcinoma cells and sensitizes these cells to sorafenib by targeting hypoxia-induced factor 1α. PLoS One 9: e115565.

Yang SL, Liu LP, Jiang JX, Xiong ZF, He QJ, Wu C (2014) The correlation of expression levels of HIF-1α and HIF-2α in hepatocellular carcinoma with capsular invasion, portal vein tumor thrombi and patients' clinical outcome. Jpn J Clin Oncol 44: 159–167

Yousefi H, Vatanmakanian M, Mahdiannasser M, Mashouri L, Alahari NV, Monjezi MR, Ilbeigi S, Alahari SK (2021) Understanding the role of integrins in breast cancer invasion, metastasis, angiogenesis, and drug resistance. Oncogene 40: 1043–1063.

Zhao Z, Zhang D, Wu F, Tu J, Song J, Xu M, Ji J (2021) Sophoridine suppresses lenvatinib-resistant hepatocellular carcinoma growth by inhibiting RAS/MEK/ERK axis via decreasing VEGFR2 expression. J Cell Mol Med 25: 549–560.

Zhu AX, Holalkere NS, Muzikansky A, Horgan K, Sahani DV (2008) Early antiangiogenic activity of bevacizumab evaluated by computed tomography perfusion scan in patients with advanced hepatocellular carcinoma. Oncologist 13: 120–125.

Zhu H, Luo SF, Wang J, Li X, Wang H, Pu WY, Zhang H, Zhuang ZX (2012) Effect of environmental factors on chemoresistance of HepG2 cells by regulating hypoxia-inducible factor-1α. Chin Med J (Engl) 125: 1095–1103.